New Soft-Switching Current Source Inverter for Photovoltaic Power System

Byung-Moon Han, Hee-Joong Kim, Seung-Taek Baek
School of Electrical & Information Control Engineering
Myongji Univ., Yongin 449-728, Korea

Abstract--This paper proposes a soft-switching current -source inverter for photovoltaic power system, which has an H-type switched-capacitor module composed of two semiconductor switches, two diodes, and an L-C resonant circuit. The operation of proposed system was analyzed by a theoretical approach with equivalent circuits and verified by computer simulations with SPICE and experimental works with a hardware prototype. The proposed system could be effectively applied for the power converter of photovoltaic power system interconnected with the power system.

Keywords--Soft Switching CSI(current source inverter), Photovoltaic System, PWM (pulse width modulation), IGBT (insulated-gate bipolar transistor), SPICE (simulation program with integrated circuit emphasis)

I. INTRODUCTION

Photovoltaic power system has been regarded the most promising future energy source among all other alternative energy sources. However, cost is still a key issue for the photovoltaic power system. One method to reduce the cost is to increase the efficiency of power converter, because it is indispensable for interfacing the photovoltaic cells with the commercial power system and load.

Voltage source inverter has been normally used as a power converter for the photovoltaic power system although photovoltaic cell has characteristics of both voltage source and current source. Main reason is that voltage source inverter has higher efficiency than the current source inverter, due to the low dissipative losses in the dc link capacitor compared with the resistive and core losses in the dc link reactor.

In this paper, a new current source inverter with soft-switching scheme is introduced for the photovoltaic power system. The basic idea is that the power converter using soft-switching current-source inverter could have higher efficiency compared with the power converter using hard-switching voltage source inverter.[7] The system is composed of a single-phase current-source inverter with an H-type soft-switching module. The operation of proposed system was analyzed in detail through theoretical approaches with equivalent circuit and computer simulations with SPICE. A scaled prototype was built and tested for verifying feasibility of hardware implementation.

II. SYSTEM CONCEPT

Current source inverter applied for the photovoltaic power system provides the following advantages.

- Utilization of current limiting characteristic of the photovoltaic cell for safe operation, due to the low short circuit current of 1.1 ~ 1.3 times the nominal current.
- No need to worry about the inrush current due to the short circuit of load and the short circuit of inverter due to the fault.
- No need to make the inverter output voltage higher than the power system voltage for interconnection.

Because of these advantages, the application of current source inverter for the photovoltaic power system has been studied by other researchers.[2,3]

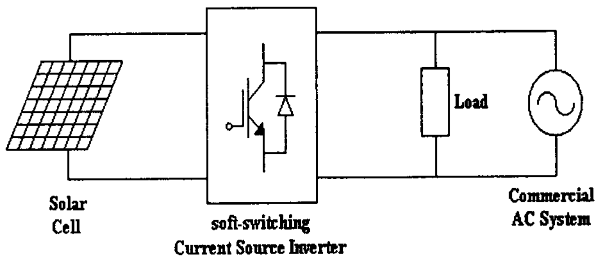

Fig. 1. Concept for photo-voltaic application

The whole system concept for the proposed photovoltaic power system is shown in Fig. 1. The major components of the system is the soft-switching current source inverter, which interfaces the solar cell output with the commercial ac load and power system.

III. CURRENT SOURCE INVERTER

The soft-switching current source inverter proposed has a single-phase current source inverter with a commutation circuit in dc side as shown in Fig. 2.

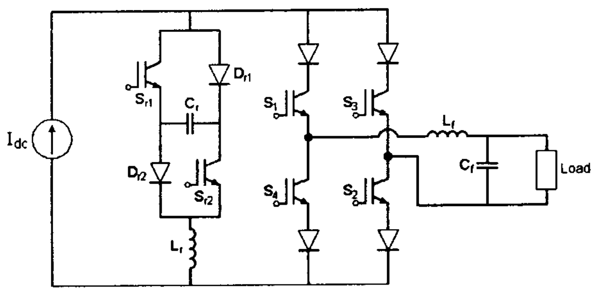

Fig. 2. Proposed current source inverter

The single-phase full bridge consists of four IGBTs connected in series with four fast-recovery diodes ($S_1/D_1 \sim S_4/D_4$). The soft-switching module consists of inductor L_r and capacitor C_r, IGBT S_{r1} and S_{r2}, and fast-recovery diode D_{r1} and D_{r2}. But the power ratings of these IGBTs and diodes are much smaller than those in the full bridge.

The commutation process of proposed compensator is divided into six operation modes. Fig. 3 shows waveforms of inductor current i_r, capacitor voltage V_C, voltage across main switches S_1, S_3, and voltage across auxiliary switches S_{r1}, S_{r2} in the commutation circuit. Fig. 4 shows equivalent circuits for six operation modes. Each operation mode was explained in detail using step by step approach, where V_m is the peak ac voltage

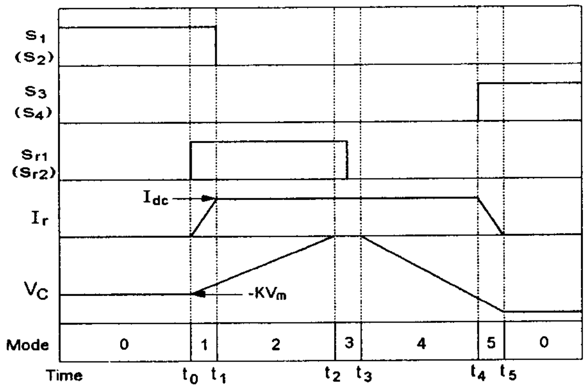

Fig. 3. Commutation operation diagram

Mode 0 – Initial state mode

It is assumed that the main current is flowing through inverter switches S_1 and S_2 and the resonant current is zero. The capacitor C_r was already charged by $-kV_m$, where k is an initial charge factor equal to about 1.3.

Mode 1 – Current build-up mode

Commutation switches S_{r1} and S_{r2} turn on in zero current state. The resonant current i_r starts to conduct and increases up to nominal reactor current I_{dc}. In this moment switch S_1 and S_2 are in zero-current mode. They are turned off by gate signals. The resonant current and capacitor voltage can be expressed as the following equation, where V_T is the ac terminal voltage at this mode.

Initial condition: $i_r = 0,\ v_C = -kV_m$

$$i_r = \frac{1}{Z_r}(kV_m + V_T)\sin\omega_r(t - t_0) \tag{1}$$

$$v_C = V_T - (kV_m + V_T)\cos\omega_r(t - t_0) \tag{2}$$

where, $Z_r = \sqrt{\frac{L_r}{C_r}}$, $\omega_r = \frac{1}{\sqrt{L_r C_r}}$

The duration of Mode 1 can be calculated as the following equation.

$$t_1 - t_0 = \frac{1}{\omega_r}\sin^{-1}\left(\frac{Z_r I_{dc}}{kV_m + V_T}\right) \tag{3}$$

The voltage across resonant capacitor at $t = t_1$ is obtained by the following equation.

$$v_C(t_1) = V_m - \sqrt{(kV_m + V_T)^2 - (Z_r I_{dc})^2} \tag{4}$$

Mode 2 – Capacitor discharge mode

In this mode there are two current paths. The dc current flows through the dc reactor. And the resonant current flows through S_{r1}, C_r, S_{r2} until resonant capacitor C_r discharges fully. The resonant current can be expressed as the following equation.

$$\begin{aligned} v_C &= \frac{1}{C_r}\int_{t_1}^{t} i_r dt + v_C(t_1) \\ &= \frac{I_{dc}}{C_r}(t - t_1) + v_C(t_1) \end{aligned} \tag{5}$$

where, $i_r = I_{dc}$

The duration of Mode 2 is obtained by the following equation.

$$\begin{aligned} t_2 - t_1 &= \frac{-C_r}{I_{dc}} v_C(t_1) \\ &= \frac{-C_r}{I_{dc}}\left(V_m - \sqrt{(kV_m + V_T)^2 - (Z_r I_{dc})^2}\right) \end{aligned} \tag{6}$$

where, $v_C(t_2) = 0$

The time elapsed for reverse voltage across the switch can be derived from equation (6) as the following.

$$\begin{aligned} t_{RV} &= \frac{C_r}{I_{dc}}(V_T - v_C(t_1)) \\ &= \frac{C_r}{I_{dc}}\sqrt{(kV_m + V_T)^2 - (Z_r I_{dc})^2} \end{aligned} \tag{7}$$

Mode 3 – Free-wheeling mode

The cell current flows through S_{r1}, D_{r1}, S_{r2}, D_{r2} through free-wheeling action. The voltage across resonant capacitor becomes zero, while the reactor current is maintained.

$$i_r = I_{dc},\ v_C = 0 \tag{8}$$

The time elapsed during this mode is negligible. So, it is assumed almost zero as the following.

$$t_3 - t_2 \cong 0 \tag{9}$$

Mode 4 – Capacitor charging mode

Switches S_{r1} and S_{r2} in soft-switching module turn off in zero voltage state. The cell current flows through D_{r1}, C_r, and D_{r2}. The capacitor C_r is slowly charged, whose voltage is expressed as the following equation.

$$i_r = I_{dc}, \quad v_C = -\frac{I_{dc}}{C_r}(t - t_3) \tag{10}$$

The time elapsed during this mode is calculated by the following equation.

$$t_4 - t_3 = \frac{C_r k V_m}{I_{dc}} \tag{11}$$

where, $v_C(t_4) = -kV_m$

Mode 5 – Current transition mode

At the end of Mode 4, the capacitor voltage is charged by $-kV_m$. Inverter switches S_3 and S_4 turn on in zero current state. The commutation circuit is blocked from the main circuit.

Initial condition: $i_r = -I_{dc}$, $v_C = -kV_m$

$$i_r = -\frac{1}{Z_r}(kV_m - V_T')\sin\omega_r(t - t_4) + I_{dc}\cos\omega_r(t - t_4) \tag{12}$$

$$v_C = V_T' + (kV_m - V_T')\cos\omega_r(t - t_4) + Z_r I_{dc}\sin\omega_r(t - t_4) \tag{13}$$

where, V_T' is the ac terminal voltage at this mode.

The duration of this current transition mode can be derived as the following equation.

$$t_5 - t_4 = \frac{1}{\omega_r}\tan^{-1}\left(\frac{Z_r I_{dc}}{kV_m - V_T'}\right) \tag{14}$$

where, $i_r(t_5) = 0$

Total commutation time can be derived by adding equation (3), (6), (9), and (11).

$$t_5 - t_0 = \frac{1}{\omega_r}\sin^{-1}\left(\frac{Z_r I_{dc}}{KV_m + V_T}\right) + \frac{1}{\omega_r}\tan^{-1}\left(\frac{Z_r I_{dc}}{kV_m - V_T'}\right) + \frac{C_r k V_m}{I_{dc}} - \frac{-C_r}{I_{dc}}\left(V_m - \sqrt{(kV_m + V_m)^2 - (Z_r I_{dc})^2}\right) \tag{15}$$

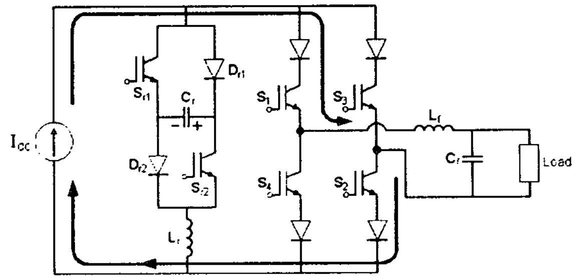

(a) mode 0

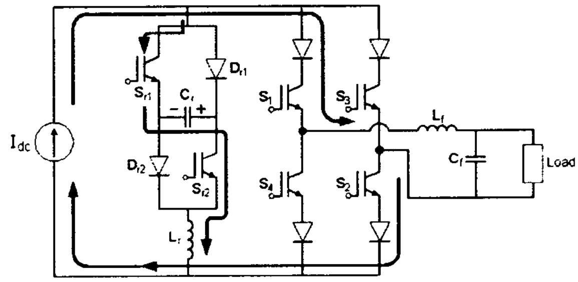

(b) mode 1

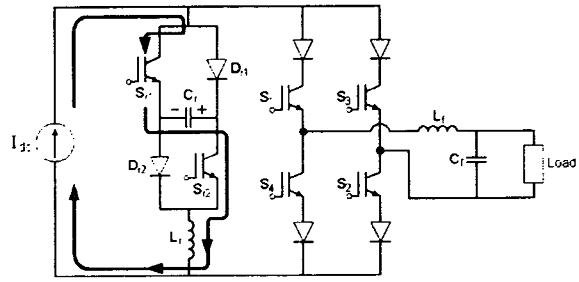

(c) mode 2

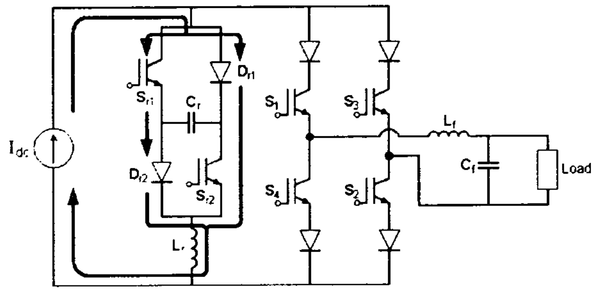

(d) mode 3

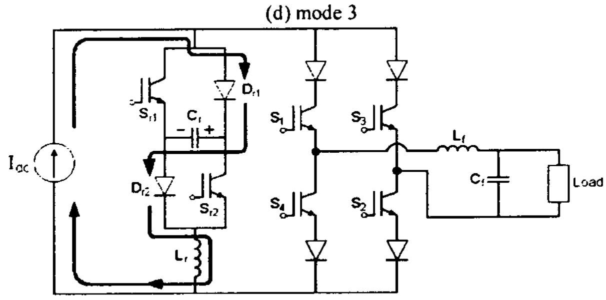

(e) mode 4

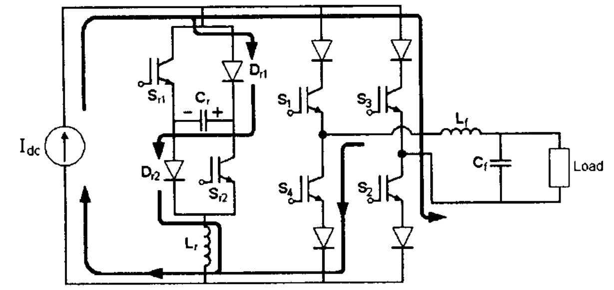

(f) mode 5

Fig. 4. Operation mode of commutation

The design of commutation circuit can be implemented considering the detail operation mechanism of each mode. The value of charge factor k for proper commutation can be determined by the following equation.

$$k \geq 1 + \frac{Z_r}{Z_m} \qquad (16)$$

where, $Z_m \equiv \frac{V_m}{I_{dc}}$

The value of C_r should be determined by considering the maximum dv/dt and di/dt of switching elements, and the maximum resonant commutation time.

The switching pattern to determine the turn-on and turn-off instance of switching element affects the harmonic level of the output current. Generally, this can be reduced, as increasing the number of pulses within a half period of power frequency. However, the maximum number of pulses is determined by the switching speed of switching element and the resonant frequency of commutation circuit.

In this study, a special switching pattern was adopted. The switches in upper part, S1and S3 operate in square wave mode, while the switches in lower part, S2and S4 operate in PWM mode. The PWM pulses are generated by comparison of the sinusoidal reference with the saw-toothed carrier as shown in Fig. 5. The pulses for switch S2 have inverting relationship with those for switch S4. The pulses for switch S2 are generated when the reference signal larger than the saw-toothed carrier for one half period. And the pulses for switch S4 are generated when the reference signal larger than the saw-toothed carrier for another half period.

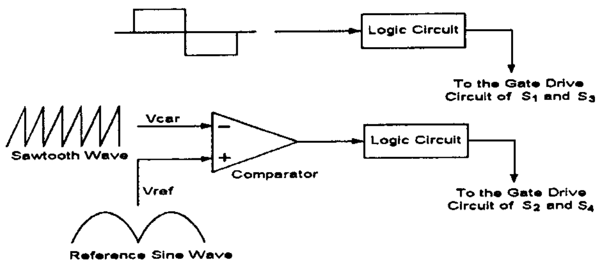

Fig. 5. Gate pulse generation

IV. SIMULATION

In order verify the proposed soft-switching current-source inverter, computer simulations with SPICE have been. The power network used in simulation is exactly same as that shown in Fig. 3. The circuit parameters used in simulation are shown in Table l.

Table 1. Simulation parameters

Source Voltage	150V $_{rms}$
AC Filter L_f, C_f	5mH, 20μF
Resonant Reactor L_r	18μH
Resonant Capacitor C_r	0.15μF
DC Reactor L_{dc}	500mH

Fig. 6 shows the simulation results. Fig. 6a shows the voltage and current waveforms, which explain the commutation operation. The upper two show the voltage across the switch S1 and S3. The third one shows the resonant pulses for Sr1 and Sr2. The fourth and fifth waveforms show the resonant current and voltage in capacitor. Fig 6b shows two sets of pulses, square pulse for switch S1and S4 and PWM pulses for switch S2and S3. Fig. 6c shows the snap-shot diagram for turn-on instance of the main switch. It is clear that the switch turns on in zero-current state. Fig. 6d shows the voltage and current variations of the switch in commutation circuit. It is clear that this switch operates in soft-switching scheme too. Fig. 6e shows the voltage and current waveforms in the output terminal of proposed inverter. Although there is some harmonics, it has an envelope of sinusoidal waveform.

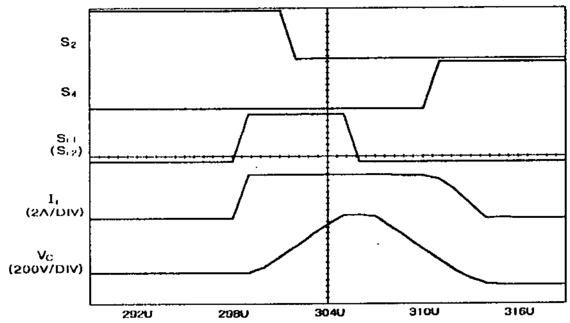

(a) commutation waveform

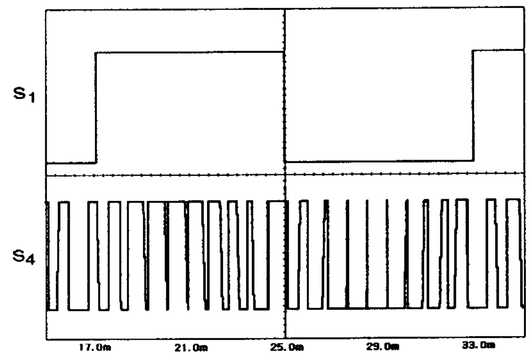

(b) pulse waveform

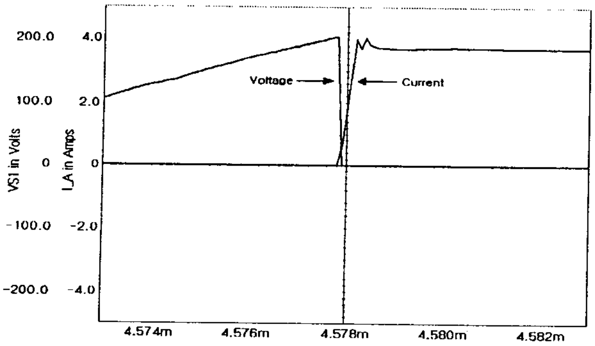

(c) turn-on transition of switch S_1

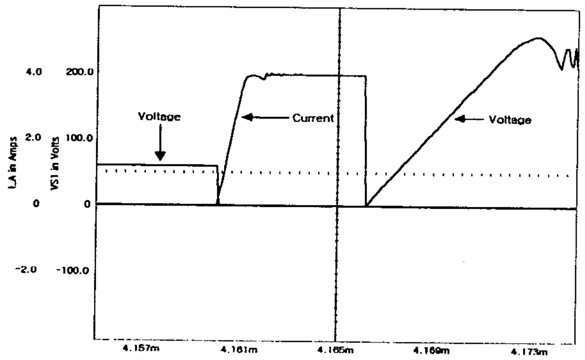

(d) turn-on and turn-off transition of S_{r1}

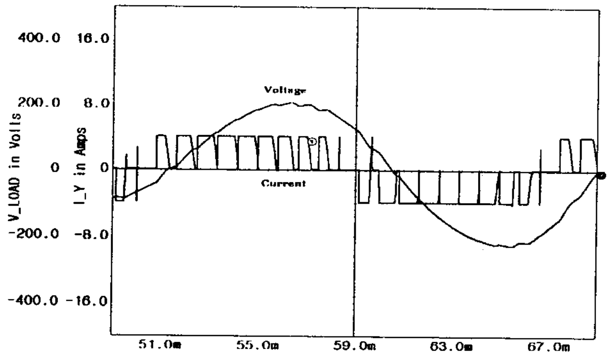

(e) output voltage and current

Fig. 6. EMTP simulation results

V. SCALED PROTOTYPE

A scaled prototype was built and tested to confirm feasibility of actual system implementation. Fig. 7 shows the circuit diagram of the scaled prototype, which has 120V/2kVA rating. The power circuit is composed of six IGBT's and six fast-recovery diodes. 80C196KC 16-bit microprocessor was used as a main controller for whole system. The bus voltage of phase A was sensed. And the sensed signal was sent to the zero-crossing detector for synchronizing the inverter output voltage with the ac system. The pulses for commutation switches are generated by detecting the falling-edge of pulses for main switches and by doing logic operation through EPLD ipLSI1032.

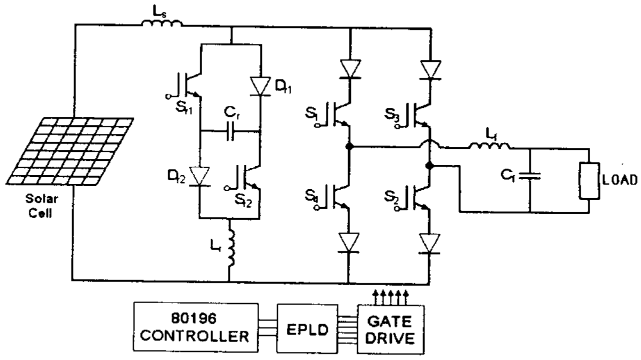

Fig. 7. Hardware configuration of scaled prototype

Fig. 8 shows the experimental results with the prototype explained above. Fig. 8a shows the voltage and current waveforms in commutation operation, which is very close to the simulation results. Fig. 8b shows two sets of pulses generated for switch S1and S3, and the PWM gate pulses generated for switch S2 and S4. Fig. 8c shows the snap-shot diagram for turn-on instance of the main switch, which is very similar shape to that in simulation.

Fig. 8d shows the voltage and current variations of the switch in commutation circuit. It is clear that this switch operates in soft-switching scheme as verified in simulation. Fig. 8e shows the output voltage and current waveforms of the proposed soft-switching inverter. Although it has some high-frequency harmonic, the output voltage has an envelope of sinusoidal wave.

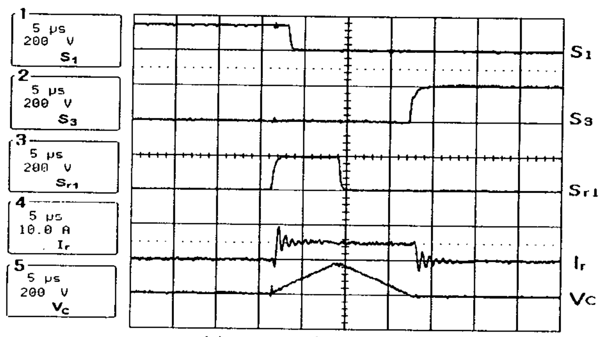

(a) commutation waveforms

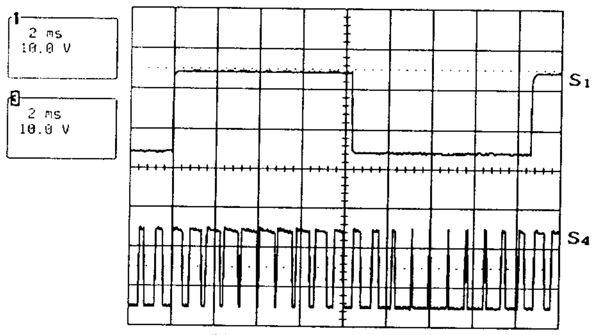

(b) pulse waveform

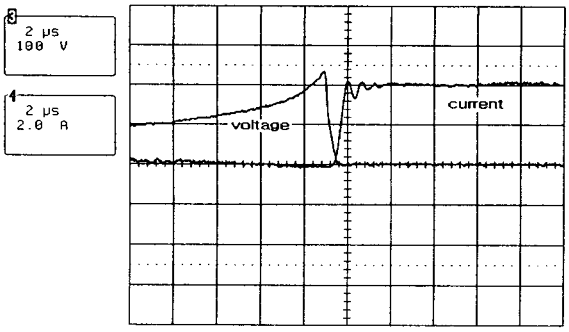

(c) turn-on transition of switch S_1

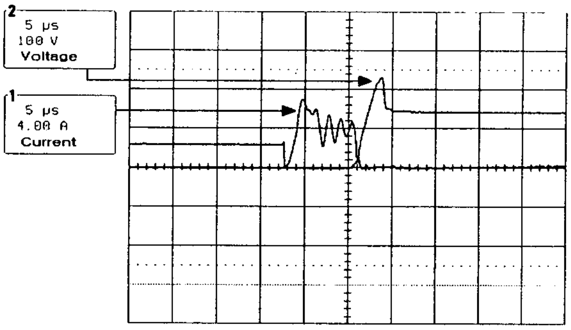

(d) turn-on and turn-off transition of S_{r1}

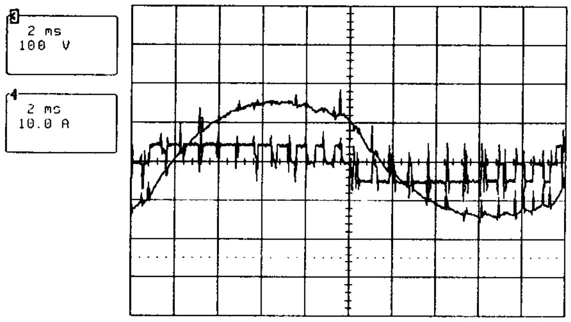

(e) output voltage and current

Fig. 8. Prototype experimental results

VI. CONCLUSION

This paper proposes a soft-switching current-source inverter with an H-type commutation module and its operation was analyzed in detail. For theoretical analysis, equivalent circuit for each operation mode was derived. And computer simulations with SPICE have been performed to confirm the system operation. A scaled prototype was also built and tested to investigate feasibility of actual system implementation.

Both simulation results and experimental results confirm that the proposed system has very low switching stress through soft-switching scheme. The low switching stress can reduce the switching loss and extend the device lifetime. The proposed soft-switching current-source inverter can be used for solar power system.

VII. REFERENCE

[1] Y.Konoshi, E.Hiraki, Y.Matsumoto, Y.L .Feng and M.Nakaoka, "Current-Fed Three-Phase Converter and Voltage-Fed Three -Phase Converter using Optimum PWM Pattern and Their Performance Evaluation", Conf. Rec. of IEEE EPE-Annual Meeting, pp. 2893 -2900, 1997.

[2] Gerry Moschopoulos and Geza Joos, "A Novel Soft-Switched PWM Current Source Rectifier / Inverter", Conf. Rec. of IEEE PESC-Annual Meeting, pp. 573 -579, 1997.

[3] K.Hirachi, K.Maysumoto, "Harmonic Current Reduction Control Scheme Single-phase Current Source-Fed PWM Inverter and Its PV System Application", Proc. PEMC'98, No.7, pp.59-64, 1998.

[4] G. Moschopoulos and G. Joos, "A Novel Soft-Switched PWM Current Source Rectifier/Inverter", Conf. Rec. of IEEE PESC-Annual Meeting, 1997, pp. 573 -579.

[5] G.Hua and F.C.Lee, "Soft-Switching Techniques in PWM Converter," IEEE IECON 1993, pp.637-643.

[6] L. D Salazar, G. Joss, "A Low Loss Soft Switching PWM CSI", PESC 1992, pp.1098 ~ 1140.

[7] S. Baek and B. Han, "New Reactive-Power Compensator using Thyristor Current Source Inverter", KIEE Trans. on Electrical Engineering, Vol. 48B, No. 4, April, 1999, pp. 219 –225.

B. Han received the B. S. degree in electrical engineering from the Seoul National University, Korea in 1976, and the M. S. and Ph.D. degree from Arizona State University in 1988 and 1992, respectively. He was with Westinghouse Electric Corporation as a senior research engineer in the Science & Technology Center. Currently he is an associate professor in the Department of Electrical Engineering at Myongji University, Korea. His research interests include the high-power power electronics and FACTS.

H. Kim was born in Seoul, Korea. He received the B. S. and Master degrees in electrical engineering from the Myongji University in 1997 and 1999 respectively. He is currently a Ph. D. candidate in the Myongji University. His research interests include power electronics application for FACTS and Custom Power.

S. Baek was born in Seoul, Korea. He received the B. S. and Master degrees in electrical engineering from the Myongji University in 1997 and 1999 respectively. He is currently a Ph. D. candidate in the Myongji University. His research interests include power electronics application for FACTS and Custom Power.